



COMPOSITE MATERIALS DYNAMIC FRACTURE STUDIES BY GENERALIZED SHMUELY DIFFERENCE ALGORITHM†

ZHU HUA and FAN TIAN-YOU

Beijing Institute of Technology, Beijing 100081, P.R. China

TIAN LAN-QIAO

Institute of Mechanics, Academia Sinica, Beijing, 100080; P.R. China

Abstract—The generalized Shmueli Difference Algorithm (GSDA) is presented here to analyze the dynamic fracture performance of orthogonal-anisotropic composite materials, such as glass fibre reinforced phenolplast. The difference recurrence formulae and boundary condition difference extrapolation formulae are derived and programmed. The dynamic stress intensity factors (DSIF) of the isotropic and anisotropic centrally cracked plates are computed respectively using GSDA and compared with that published previously. GSDA is proved effective and reliable. Copyright © 1996 Elsevier Science Ltd.

INTRODUCTION

COMPOSITE MATERIALS have been extensively employed in many fields of mechanical, aeronautical and aerospace industries etc., e.g. the space vehicle's shell and the ship's erosion resistant shell. Structural components such as these frequently experience dynamic loading. For their safe and proper service, knowledge in the mechanical performance of composite substances under high rate loading is of high necessity. The initiation and propagation of crack in composite materials, among mechanical performance of this kind, are of considerable importance, for they are crucial in structure failure prediction. For the dynamic crack initiation and crack propagation, the dynamic stress intensity factor (DSIF) plays a key role in characterizing this behaviour. Thus, the accurate determination of the DSIF in predicting fracture cannot be overemphasized.

The finite difference method has evolved as an accurate numerical method for solving a wide class of engineering problems. The first successful application of this method to calculate DSIF in dynamic fracture mechanics problems is credited to Chen [1]. Among the pioneering workers are Shmueli *et al.* [2], also. Besides the finite difference method, the finite element method and boundary element method have also been developed for calculating DSIF successfully. For a detailed discussion, interested readers are referred to refs [3–5] and Fan and Hahn [4] and Israil [5].

While the finite difference method and boundary element method have been some what of a success in calculating the DSIF of isotropic bodies, none of them has been so far employed fruitfully for DSIF of anisotropic bodies such as composite materials.

In the paper, the Generalized Shmueli Difference Algorithm (GSDA) is presented and applied to calculate the DSIF of anisotropic bodies, including the substitution of a rectangular difference grid for the square one, the derivation of a series of relevant difference recurrence formulae and boundary condition difference extrapolation formulae and the empirical establishment of criteria for stability of the difference scheme. The DSIF is computed from the crack tip stress σ_r . Centrally cracked plates subjected to uni-axial tension of Heaviside-function time-dependence are analyzed respectively in the cases of both isotropy and anisotropy. The results obtained for the case of isotropy from the present analysis are compared with the available published results. The comparison shows GSDA presented herein is credential and applicable. The results for the anisotropic case are also compared with those of the isotropic one.

†This work was supported by the grant of the Opening Laboratory of Nonlinear continuous Mechanics in Institute of Mechanics of Academia Sinica.

FUNDAMENTAL EQUATIONS

Strictly speaking, fibre reinforced resin–matrix composite materials are heterogeneous anisotropic, which can, however, be considered as homogeneous materials with anisotropy under many circumstances.

The dynamic equilibrium and strain equations for orthogonal-anisotropic bodies are the same as the isotropic ones, with the only exception being the generalized Hooke's Law. This law for the planar case can be written as [6]

$$\begin{aligned}\sigma_{xx} &= c_{11}\varepsilon_{xx} + c_{12}\varepsilon_{yy} \\ \sigma_{yy} &= c_{12}\varepsilon_{xx} + c_{22}\varepsilon_{yy} \\ \sigma_{xy} &= c_{66}\gamma_{xy},\end{aligned}\quad (1a)$$

where

$$\begin{aligned}c_{11} &= \frac{E_{11}}{1 - \nu_{12}\nu_{21}}, \quad c_{22} = \frac{E_{22}}{1 - \nu_{12}\nu_{21}} \\ c_{12} &= \frac{E_{11}\nu_{21}}{1 - \nu_{12}\nu_{21}} = \frac{E_{22}\nu_{12}}{1 - \nu_{12}\nu_{21}} \\ c_{66} &= G_{12} = G_{21},\end{aligned}\quad (1b)$$

where E_{11} and E_{22} are the moduli of elasticity in the principal directions x and y , respectively; G_{12} ($=G_{21}$) is the shear modulus, and ν_{12} and ν_{21} are Poisson's ratios in the xy -plane.

The planar orthogonal-anisotropic elastodynamic equations were derived from the dynamic equilibrium and strain equations as well as the generalized Hooke's Law. Here are:

$$\begin{aligned}c_{11}\frac{\partial^2 u}{\partial x^2} + c_{66}\frac{\partial^2 u}{\partial y^2} + (c_{12} + c_{66})\frac{\partial^2 v}{\partial x\partial y} &= \rho\frac{\partial^2 u}{\partial t^2} + \theta\rho\frac{\partial u}{\partial t} \\ c_{66}\frac{\partial^2 v}{\partial x^2} + c_{22}\frac{\partial^2 v}{\partial y^2} + (c_{12} + c_{66})\frac{\partial^2 u}{\partial x\partial y} &= \rho\frac{\partial^2 v}{\partial t^2} + \theta\rho\frac{\partial v}{\partial t},\end{aligned}\quad (2)$$

where

$$\theta\rho\frac{\partial u}{\partial t} \quad \text{and} \quad \theta\rho\frac{\partial v}{\partial t}$$

are artificial damp terms to make eq. (2) valid for statics problems. θ is the so-called subjectively damp coefficient. Equation (2) will be reduced to the orthogonal-anisotropic elasto-dynamic ones without damp, providing θ is equal to zero.

GENERALIZED SHMUELY DIFFERENCE ALGORITHM

Consider a centrally cracked plate as shown in Fig. 1. It is enough that only one-quarter of the plates is analyzed because of their symmetry (Fig. 2). When analyzing anisotropic problems, the square difference grid, used in the Shmuely Difference Algorithm [2,7], has not been applicable because of the elastic wave speed difference along the x and y axes. To solve the problem of anisotropy, the rectangular difference grid has supplanted the square one shown in Fig. 3 and the relevant difference recurrence formulae have also changed correspondingly. The so-called Generalized Shmuely Difference Algorithm has thus been developed. With the central difference discretization, eq. (2) takes the recurrence form as follows:

$$\begin{aligned}u(x, y, t + \Delta t) &= \frac{1}{1 + 0.5\theta\Delta t} \left\{ 2 \left(1 - \frac{c_{11}\Delta t^2}{\rho\Delta x^2} - \frac{c_{66}\Delta t^2}{\rho\Delta y^2} \right) u(x, y, t) \right. \\ &\quad \left. - (1 - 0.5\theta\Delta t)u(x, y, t - \Delta t) + \frac{c_{11}\Delta t^2}{\rho\Delta x^2} [u(x + \Delta x, y, t) + u(x - \Delta x, y, t)] \right\}\end{aligned}$$

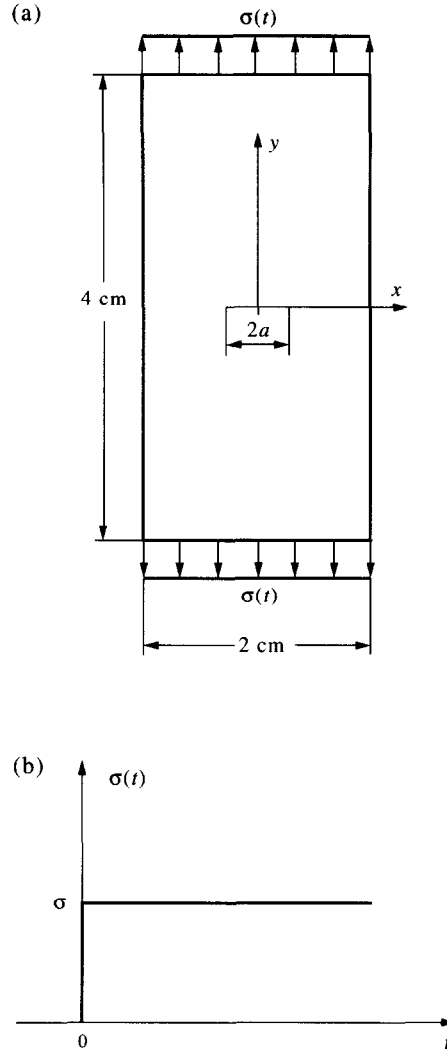


Fig. 1. (a) Centrally cracked rectangular plate. (b) Uniform tension $\sigma(t)$ with Heaviside-function time dependence.

$$\begin{aligned}
 & + \frac{c_{66}\Delta t^2}{\rho \Delta y^2} [u(x, y + \Delta y, t) + u(x, y - \Delta y, t)] \\
 & + \frac{(c_{12} + c_{66})\Delta t^2}{4\rho\Delta x\Delta y} [v(x + \Delta x, y + \Delta y, t) + v(x - \Delta x, y - \Delta y, t) \\
 & - v(x + \Delta x, y - \Delta y, t) - v(x - \Delta x, y + \Delta y, t)] \Big\} \quad (3a)
 \end{aligned}$$

$$\begin{aligned}
 v(x, y, t + \Delta t) = & \frac{1}{1 + 0.5\theta\Delta t} \Big\{ 2 \left(1 - \frac{c_{66}\Delta t^2}{\rho \Delta x^2} - \frac{c_{22}\Delta t^2}{\rho \Delta y^2} \right) v(x, y, t) \\
 & - (1 - 0.5\theta\Delta t)v(x, y, t - \Delta t) + \frac{c_{66}\Delta t^2}{\rho \Delta x^2} [v(x + \Delta x, y, t) + v(x - \Delta x, y, t)] \\
 & + \frac{c_{22}\Delta t^2}{\rho \Delta y^2} [v(x, y + \Delta y, t) + v(x, y - \Delta y, t)] + \frac{(c_{12} + c_{66})\Delta t^2}{4\rho\Delta x\Delta y} \\
 & \times [u(x + \Delta x, y + \Delta y, t) + u(x - \Delta x, y - \Delta y, t) - u(x + \Delta x, y - \Delta y, t) \\
 & - u(x - \Delta x, y + \Delta y, t)] \Big\}, \quad (3b)
 \end{aligned}$$

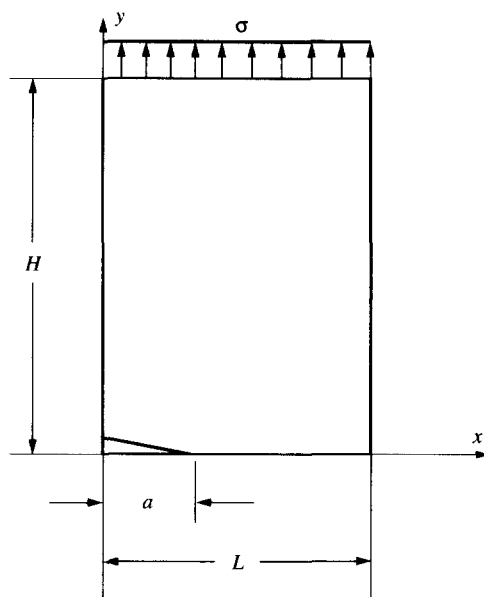


Fig. 2. One-quarter of the centrally cracked rectangular plate.

where Δt is the time interval; Δx , Δy , the grid interval along the x , y axes, respectively, as shown in Fig. 3.

BOUNDARY CONDITIONS AND THEIR DIFFERENCE FORMULAE

Figure 2 shows the boundary states of one-quarter of a centrally cracked plane and the boundary condition can be stated below:

$$\begin{aligned}
 x = L, 0 \leq y \leq H: \sigma_{xy} &= 0, \sigma_{xx} = 0 \\
 y = 0, 0 \leq x < a: \sigma_{xy} &= 0, \sigma_{yy} = 0 \\
 y = 0, a \leq x \leq L: \sigma_{xy} &= 0, v = 0 \\
 x = 0, 0 \leq y \leq H: \sigma_{xy} &= 0, u = 0 \\
 y = H, 0 \leq x < L: \sigma_{xy} &= 0, \sigma_{yy} = \sigma(t).
 \end{aligned} \tag{4}$$

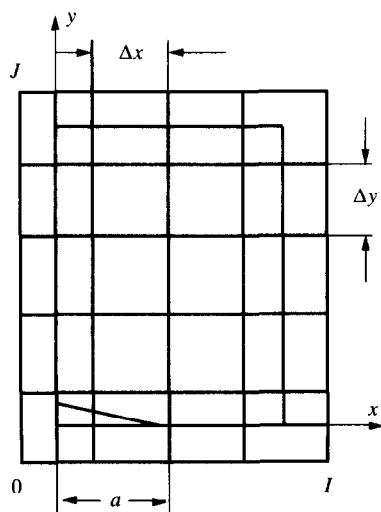


Fig. 3. Rectangular difference grid.

In Fig. 4, the grid points are numbered, where the boundary has been considered as three parts: “Sides”, “Angles” and “Angle-points” for the sake of the central difference format. So the boundary conditions [eq. (4)] can be discretized as extrapolation formulae as follows:

The extrapolation formulae for the “Sides” boundary conditions

Take “Side-1” for example:

$$u\left(L + \frac{\Delta x}{2}, y, t\right) = u\left(L - \frac{\Delta x}{2}, y, t\right) - 0.5 \frac{\Delta x}{\Delta y} \frac{c_{12}}{c_{11}} \left[v\left(L - \frac{\Delta x}{2}, y + \Delta y, t\right) - v\left(L - \frac{\Delta x}{2}, y - \Delta y, t\right) \right] \quad (5a)$$

$$v\left(L + \frac{\Delta x}{2}, y, t\right) = v\left(L - \frac{\Delta x}{2}, y, t\right) - 0.5 \frac{\Delta x}{\Delta y} \left[u\left(L - \frac{\Delta x}{2}, y + \Delta y, t\right) - u\left(L - \frac{\Delta x}{2}, y - \Delta y, t\right) \right] \\ y = 3\Delta y, \dots, (n-2)\Delta y. \quad (5b)$$

The extrapolation formulae for the “Angle” boundary conditions

Take “Angle-1” for example:

$$u\left(L - \frac{\Delta x}{2}, -\frac{\Delta y}{2}, t\right) = \frac{1}{1 - 0.5^2} \left\{ u\left(L - \frac{\Delta x}{2}, \frac{\Delta y}{2}, t\right) - 0.5^2 u\left(L - \frac{\Delta x}{2}, \frac{3\Delta y}{2}, t\right) \right. \\ \left. + 0.5 \frac{\Delta y}{\Delta x} \left[v\left(L - \frac{\Delta x}{2}, \frac{\Delta y}{2}, t\right) - v\left(L - \frac{3\Delta x}{2}, \frac{\Delta y}{2}, t\right) \right] \right\} \quad (6a)$$

$$v\left(L + \frac{\Delta x}{2}, \frac{\Delta y}{2}, t\right) = \frac{1}{1 - 0.5^2} \left\{ v\left(L - \frac{\Delta x}{2}, \frac{\Delta y}{2}, t\right) - 0.5^2 v\left(L - \frac{3\Delta x}{2}, \frac{\Delta y}{2}, t\right) \right. \\ \left. + 0.5 \frac{\Delta x}{\Delta y} \left[u\left(L - \frac{\Delta x}{2}, \frac{\Delta y}{2}, t\right) - u\left(L - \frac{\Delta x}{2}, \frac{3\Delta y}{2}, t\right) \right] \right\} \quad (6b)$$

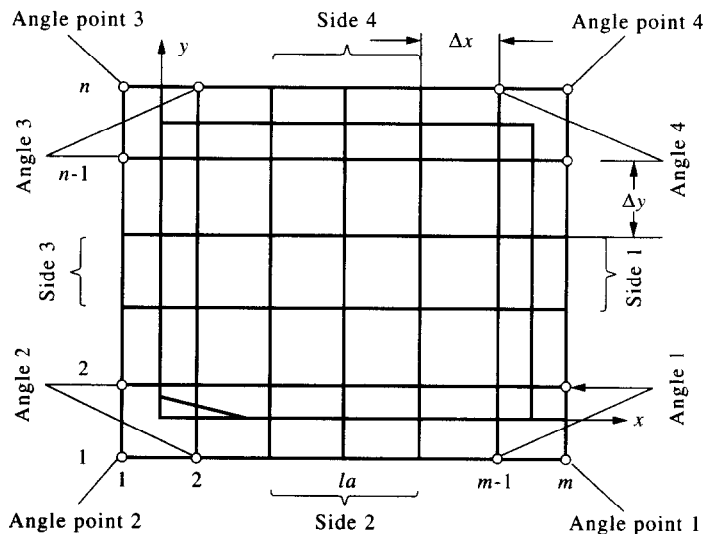


Fig. 4. “Sides”, “Angles” and “Angle-points”.

$$u\left(L + \frac{\Delta x}{2}, \frac{\Delta y}{2}, t\right) = u\left(L - \frac{\Delta x}{2}, \frac{\Delta y}{2}, t\right) + 0.5 \frac{\Delta x}{\Delta y} \frac{c_{12}}{c_{11}} \left[v\left(L - \frac{\Delta x}{2}, \frac{3\Delta y}{2}, t\right) + v\left(L - \frac{\Delta x}{2}, \frac{\Delta y}{2}, t\right) \right] \quad (6c)$$

$$v\left(L - \frac{\Delta x}{2}, -\frac{\Delta y}{2}, t\right) = -v\left(L - \frac{\Delta x}{2}, \frac{\Delta y}{2}, t\right). \quad (6d)$$

The extrapolation formulae for the “Angle-points” boundary conditions

The displacements of the four “angle-points”

$$\left(-\frac{\Delta x}{2}, -\frac{\Delta y}{2}\right), \left(-\frac{\Delta x}{2}, H + \frac{\Delta y}{2}\right), \left(L + \frac{\Delta x}{2}, H + \frac{\Delta y}{2}\right), \left(L + \frac{\Delta x}{2}, -\frac{\Delta y}{2}\right),$$

can be obtained using linear extrapolation based on the other two grid points located on the two grid lines orthogonal to the angular points. For instance, the extrapolation formulae for the “angle-point”

$$\left(-\frac{\Delta x}{2}, \frac{\Delta y}{2}\right)$$

are given as

$$u\left(-\frac{\Delta x}{2}, -\frac{\Delta y}{2}, t\right) = u\left(\frac{\Delta x}{2}, -\frac{\Delta y}{2}, t\right) + u\left(-\frac{\Delta x}{2}, \frac{\Delta y}{2}, t\right) - 0.5 \left[u\left(-\frac{3\Delta x}{2}, -\frac{\Delta y}{2}, t\right) - u\left(-\frac{\Delta x}{2}, \frac{3\Delta y}{2}, t\right) \right] \quad (7a)$$

$$v\left(-\frac{\Delta x}{2}, -\frac{\Delta y}{2}, t\right) = v\left(\frac{\Delta x}{2}, -\frac{\Delta y}{2}, t\right) + v\left(-\frac{\Delta x}{2}, \frac{\Delta y}{2}, t\right) - 0.5 \left[v\left(-\frac{3\Delta x}{2}, -\frac{\Delta y}{2}, t\right) - v\left(-\frac{\Delta x}{2}, \frac{3\Delta y}{2}, t\right) \right]. \quad (7b)$$

CRITERIA FOR STABILITY OF THE DIFFERENCE SCHEME

It is necessary to provide the criteria for stability of the difference format so as to make valid the difference extrapolation formulae this paper presented. Via repeating computation, we suggest the criteria take the form:

$$\frac{\Delta t}{\Delta x} \sqrt{c_{11}/\rho} < 0.86, \quad \frac{\Delta t}{\Delta y} \sqrt{c_{22}/\rho} < 0.86. \quad (8)$$

Furthermore, it is best to take

$$\frac{\Delta t}{\Delta x} \sqrt{c_{11}/\rho} = 0.80, \quad \frac{\Delta t}{\Delta y} \sqrt{c_{22}/\rho} = 0.80. \quad (9)$$

DYNAMIC STRESS INTENSITY FACTOR

Because the singularity at the crack tip in the dynamic case can be considered as being similar to the static case before the crack begins to propagate, the DSIF can be defined as the same in

a static problem except for its being time-dependent. It can be determined as before from the crack tip stress σ_{yy} [4]. Only valid for mode I:

$$\sigma_{yy} = \frac{K_I(t)}{\sqrt{2\pi r}} f(\theta), \quad (10a)$$

where

$$f(\theta) = \operatorname{Re} \left\{ \frac{1}{s_1 - s_2} \right\} \left[\frac{s_1}{\sqrt{\cos\theta + s_2 \sin\theta}} - \frac{s_2}{\sqrt{\cos\theta + s_1 \sin\theta}} \right]. \quad (10b)$$

$s_1, \bar{s}_1, s_2, \bar{s}_2$ with the overbar designating complex conjugates are the roots of the equation below:

$$s^4 + \left(\frac{E_{11}}{G_{12}} - 2\nu_{12} \right) s^2 + \frac{E_{11}}{E_{22}} = 0. \quad (11)$$

Due to any finite difference method being unable to represent the extremely steep stress gradients occurring in the neighbourhood of a crack tip, the extrapolation of the mode I DSIF $K_I(t)$ from the stress field in the vicinity of the crack tip is used here.

EXAMPLES

Isotropic centrally cracked plate

To justify the GSDA proposed, a detailed investigation was made into the isotropic centrally cracked plates [Fig. 1(a)]. Included are comparisons with previously published results. The plate is loaded dynamically in the y axial direction by a uniform tension $\sigma(t)$ with Heaviside-function time dependence [Fig. 1(b)] and its boundary conditions are given corresponding to plane loading. The various dimensions of the plate and the relevant material properties are [1]:

$$2H = 40 \text{ mm}$$

$$2L = 20 \text{ mm}$$

$$a = 2.4 \text{ mm}$$

Young's modulus:

$$E_{11} = E_{22} = 2.00 \times 10^5 \text{ MPa}$$

$$G_{12} = G_{21} = 7.69 \times 10^4 \text{ MPa}$$

Poisson's ratio

$$\nu_{12} = \nu_{21} = 0.30$$

Density

$$\rho = 5.00 \times 10^3 \text{ kg/m}^3.$$

The normalized mode I DSIF $K_I(t)/\sigma\sqrt{\pi a}$ from the present analysis is plotted against t in Fig. 5(a). The published results of Chen [1], Maue [8], and Murti and Valliappan [9] are in Fig. 5(b). Through comparison, it is plain that the authors agree with their forerunners, in particular perfectly with Murti's solution, but there still exists a little difference at the initial time interval. So the conclusion is that the GSDA is sound and reliable.

Anisotropic centrally cracked plate

Take an anisotropic centrally cracked plate [Fig. 1(a)] with various dimensions and its material properties listed below [8]:

$$2H = 40 \text{ mm}$$

$$2L = 20 \text{ mm}$$

$$a = 2.4 \text{ mm}$$

Young's modulus:

$$\begin{aligned} E_{11} &= 1.83 \times 10^4 \text{ MPa}, \\ E_{22} &= 5.48 \times 10^4 \text{ MPa} \\ G_{12} &= G_{21} = 8.79 \times 10^3 \text{ MPa} \end{aligned}$$

Poisson's ratio:

$$\nu_{12} = 0.083, \nu_{21} = 0.25$$

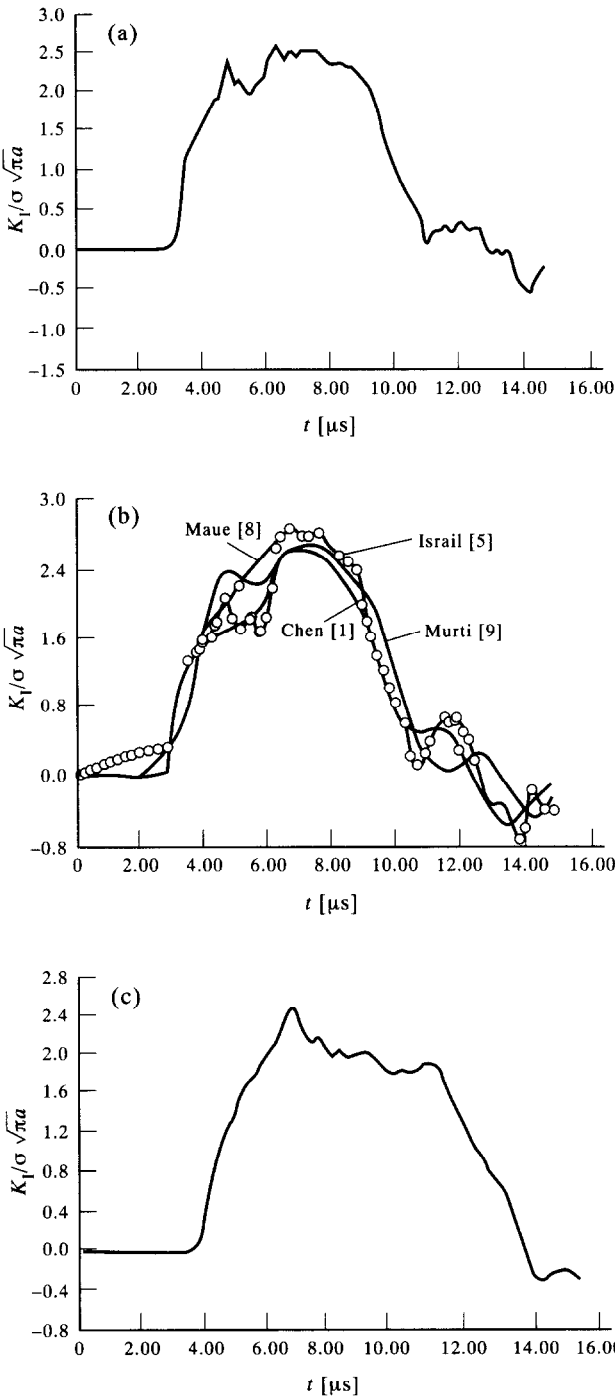


Fig. 5. (a) Normalized mode I DSIF of isotropic centrally cracked plate from GSDA. (b) Published normalized mode I DSIF of isotropic centrally cracked plate. (c) Normalized mode I DSIF of anisotropic centrally cracked plate from GSDA.

Density:

$$\rho = 1.90 \times 10^3 \text{ kg/m}^3.$$

The normalized mode I DSIF for orthogonal anisotropic bodies is, by the GSDA, shown in Fig. 5(c) and compared with that of an isotropic plate. One can easily find that the $K_I(t)$ curve descends more smoothly for orthogonal-anisotropic than for isotropic after it passes its peak value.

CONCLUSIONS

The generalized Shmueli difference algorithm is proposed to investigate dynamic fracture problems with orthogonal-anisotropic composite materials, such as glass fibre reinforced phenoplast. As a result of the extent of the difference of speeds of elastic waves along the x and y axes in orthogonal-anisotropic materials, a rectangular grid should be applied in place of the square one used by Shmueli. Then the relationships between the Δx and Δy in the rectangular grid and Δt are established for computational stability.

The dynamic stress intensity factor for an isotropic centrally cracked plate is obtained by GSDA and compared with the published ones. The comparison has confirmed the effectiveness and reliability of GSDA.

Applying GSDA, the DSIF for orthogonal-anisotropic centrally cracked plates has been, for the first time, obtained. By comparing the DSIF for orthogonal-anisotropic bodies with that for isotropic ones, one can easily find that the $K_I(t)$ curve descends more smoothly for orthogonal-anisotropic than for isotropic after it passes its peak value.

For difference boundary conditions, this paper presented the approach of dividing the boundary into three portions, i.e. "Side", "Angle" and "Angle-point". The theoretical analysis and computation demonstrate that the approach is applicable.

REFERENCES

- [1] Y. M. Chen, Numerical computation of dynamic stress intensity factors by a Lagrangian finite-difference method. *Engng Fracture Mech.* **7**, 653–660 (1975).
- [2] M. Shmueli *et al.*, Static and dynamic analysis of the DCB problem in fracture mechanics. *Int. J. Solids Structures* **12**, 67–79 (1976).
- [3] M. F. Kanninen, A critical appraisal of solution techniques in dynamic fracture mechanics, in *Numerical Method of Fracture Mechanics* (Edited by A. R. Luxmore and D. R. J. Owen), pp. 612–634. Pineridge Press, Swansea.
- [4] T. Y. Fan and H. G. Hahn, An application of boundary integral equation method to dynamic fracture mechanics. *Engng Fracture Mech.* **21**, 307–313 (1985).
- [5] A. S. M. Israil and G. F. Dargush, Dynamic fracture mechanics studies by time-domain BEM. *Engng Fracture Mech.* **39**, 315–328 (1991).
- [6] *Mechanics of Fracture* (Edited by G. C. Sih), Vol. 6. Nordhoff International Publishing, Leyden (1980).
- [7] T. Y. Fan, *An Introduction to Dynamic Fracture Mechanics*. Press of Beijing Institute of Technology, Beijing (1990) (in Chinese).
- [8] A. W. Maue, *Zeitschrift für angewandte. Math. Mech.* **34**, 1–12 (1954).
- [9] V. Murti and S. Valliappan, The use of quarter point element in dynamic crack analysis. *Engng Fracture Mech.* **23**, 585–614 (1986).

(Received 14 July 1994)